Supporting Information

Harvesting Mechanical Energy for Hydrogen Generation by Piezoelectric Metal–Organic Frameworks

Shiyin Zhao, Maosong Liu, Yuqiao Zhang, Zhicheng Zhao, Qingzhe Zhang, Zhenliang Mu, Yangke Long, Yinhua Jiang, Yong Liu, Jianming Zhang, Shun Li, Xuanjun Zhang,* and Zuotai Zhang**

Experimental

Chemicals: Zirconium chloride ($ZrCl_4$), glacial acetic acid (HAc), and sulfite (Na_2SO_3) were purchased from Macklin Agents (Shanghai, China). Terephthalic acid (BDC) and 2,3,5,6-tetrafluoroterephthlonic acid (BDC-F_4) were purchased from Yanshen Technology Co., Ltd. (Jilin, China). N,N-dimethylformamide (DMF), ethanol and methanol were used as solvents purchased from Anaqua Global International Inc., Ltd (Cleveland, USA). All the agents were used as received without any further purification.

Preparation of UiO-66(Zr) type MOFs: The microwave-assisted hydrothermal method was employed to assemble the UiO-66 type MOFs. For the synthesis of UiO-66, 75 mg $ZrCl_4$, 3.66 mL HAc and 20 mL DMF were mixed in a Teflon container (120 mL) and sonicated for 5 min. Afterward, 60 mg BDC was added in the above mixture followed by ultrasonication for 10 min. Then the Teflon reactor was moved to a microwave oven and heated at 100 ℃ for 4 h. After cooling down to room temperature, the as-obtained precipitate was washed by DMF and ethanol for several times followed by drying in a vacuum oven at 80 ℃ for 8 h.

The UiO-66-F_4 was assembled by a similar method. In a typical experiment, 85.9 mg BDC-F_4 was added in 50 mL a mixed solution of water/HAc (30/20). After 5 min of sonication, 75 mg $ZrCl_4$ was added and then sonicated for 10 min. Afterward, the mixed solution was moved to the microwave oven and heated at 100 ℃ for 4 h. After cooling down to room temperature, the as-obtained precipitate was washed by DMF and ethanol for several times followed by drying in a vacuum oven at 80 ℃ for 8 h.

Characterizations*:* The crystal structure was investigated by powder X-ray Diffraction (XRD, Rigaku) with Cu K_α radiation. The morphology and crystal structure were analyzed by field emission scanning electron microscope (SEM, Zeiss, Merlin) and high-resolution transmission electron microscope (TEM, Talos F200i, Thermo Scientific). The Fourier-transform infrared (FTIR) spectra were measured by a Nicolet iS50 spectrometer with KBr pellets. The X-ray photoelectron spectroscopy (XPS) were recorded on a Thermo Scientific

ESCALAB 250XI with Al K_α irradiation source. All the binding energies were referenced to the C1s peak at 284.6 eV. The specific surface areas and pore size distributions were analyzed through a surface area and porosimetry analyzer (Micromeritics ASAP 2460). The photoluminescence spetra were collected using an Edinburgh FLS1000 fluorescence spectrophotometer with an excitation wavelength of 500 nm. The diffuse reflectance spectra (DRS) were recorded on PerkinElmer Lambda 750 UV-vis spectroscopy. The piezoresponse force microscopy (PFM) measurements were conducted using Bruker-Icon with a working probe of MESP (~2 N/m, resonance frequency of 75 Hz).

***Hydrogen evolution and electrochemical measurements**:* The piezocatalytic H_2 production measurements were performed in a Pyrex reaction cell connected to a closed gas circulation system (Labsolar-6A, Beijing Perfectlight Co., Ltd.). An ultrasonic cleaner (Branson 2800) with a maximum power of 110 W and a frequency of 40 kHz was used to periodically apply a local mechanical strain on the samples. In a typical test, 20 mg powder sample was dispersed in a quartz reaction vessel containing 15 mL Na_2SO_3 (1 mol/L) and 85 mL distilled water. The amounts of generated H_2 were determined using a gas chromatography (Techcomp GC-7900).

The electrochemical measurements were carried out on a CHI 760E electrochemical workstation in a standard three-electrode system with MOFs-coated ITO as the working electrode, Pt plate as the counter electrode, and Ag/AgCl as a reference electrode. A 0.1 M Na_2SO_4 deoxygenated aqueous solution was used as the electrolyte. The concentration of KCl in Ag/AgCl electrode is 3 mol/L. The electrochemical impedance spectra (EIS) measurements were performed with a bias potential of –1.4 V. The disturbance voltage is 5 mV, and the frequency for the EIS measurements is 1000 Hz. The Mott–Schottky plots were measured at frequencies of 500, 1000, and 1500 Hz, respectively.

***DFT simulations**:* First-principles calculations were carried out using density functional theory (DFT) with generalized gradient approximation (GGA) of Perdew-Burke-Ernzerhof (PBE) implemented in the Vienna Ab-Initio Simulation Package (VASP). The valence

electronic states were expanded on the basis of plane waves with the core-valence interaction represented using the projector augmented plane wave (PAW) approach and a cutoff of 520 eV. A Γ-centered k-mesh of 1×1×1 was used for the surface calculations. Convergence is achieved when the forces acting on ions become smaller than 0.02 eV/Å.

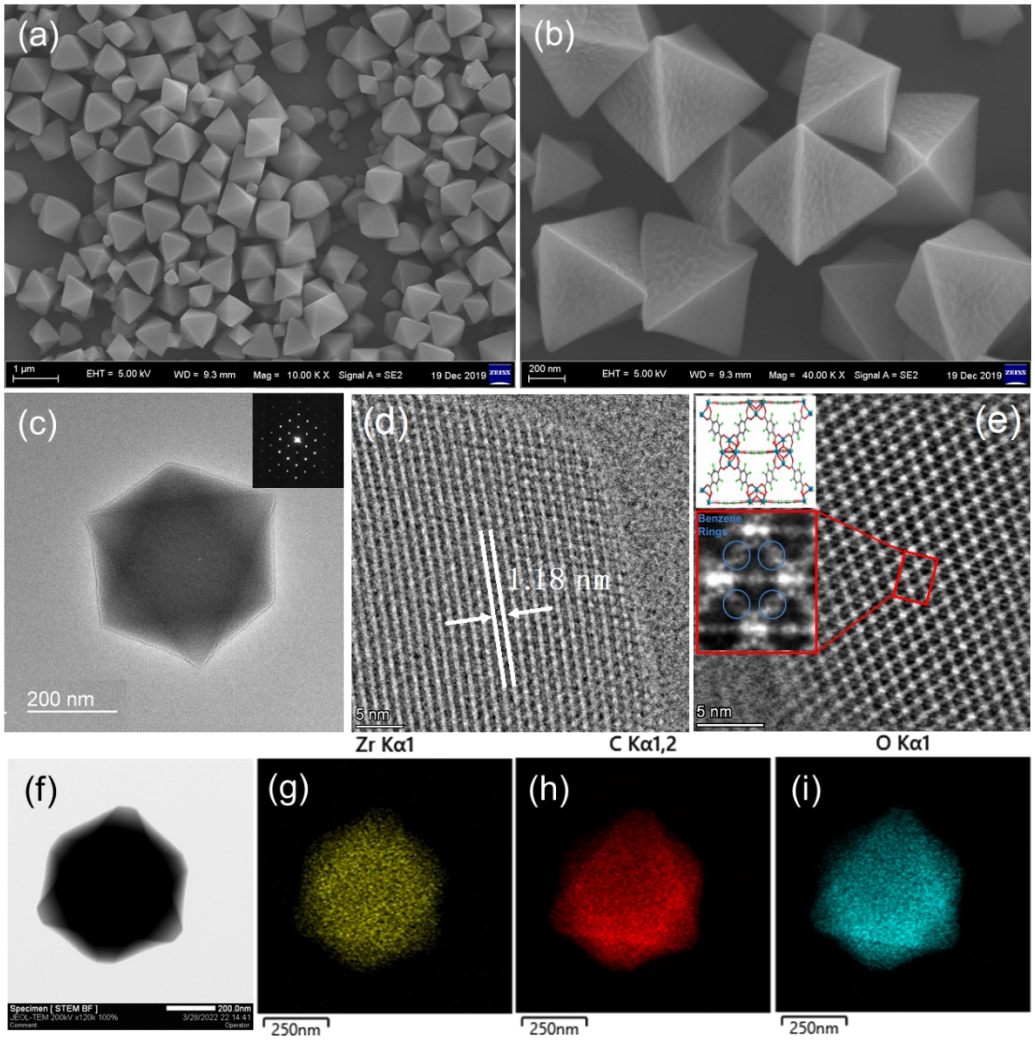

Figure S1. (a and b) SEM, (c) TEM (inset shows the SAED patterns), (d) high-resolution TEM, and (e) STEM iDPC image and corresponding crystal structure of the UiO-66 MOF. (f) HAADF-STEM and EDS mapping images of (g) Zr, (h) C and (i) O elements.

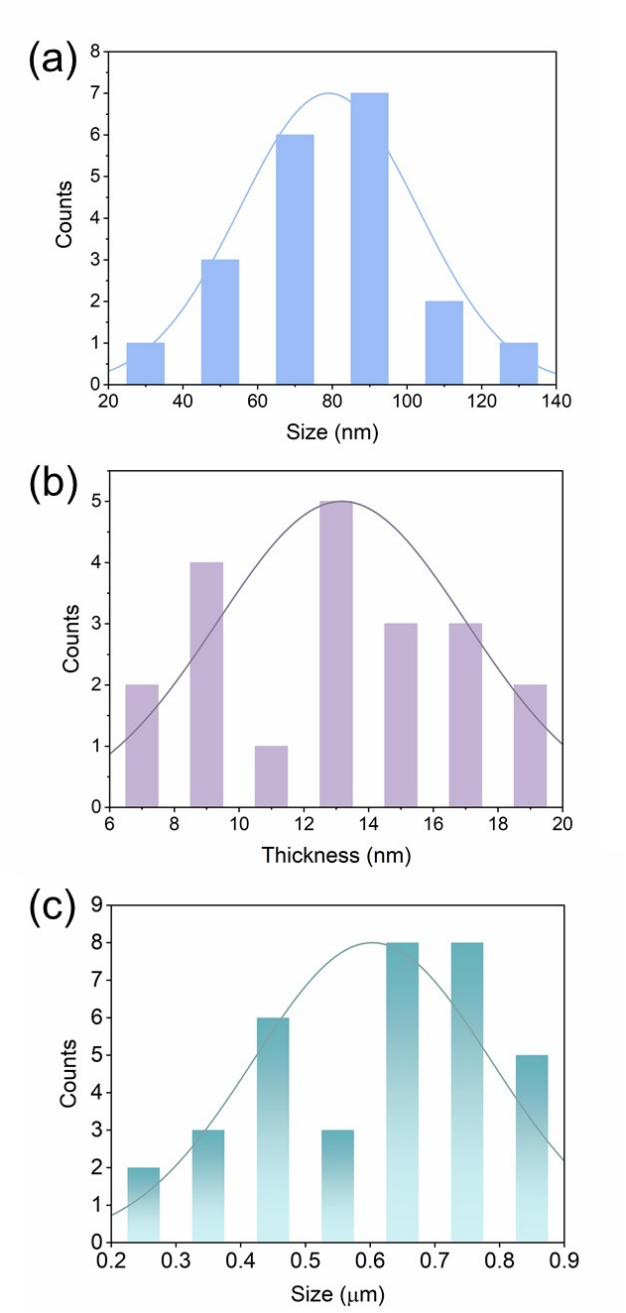

Figure S2. (a) Size and (b) thickness distributions of UiO-66-F_4 nanosheets. (c) Size distributions of UiO-66.

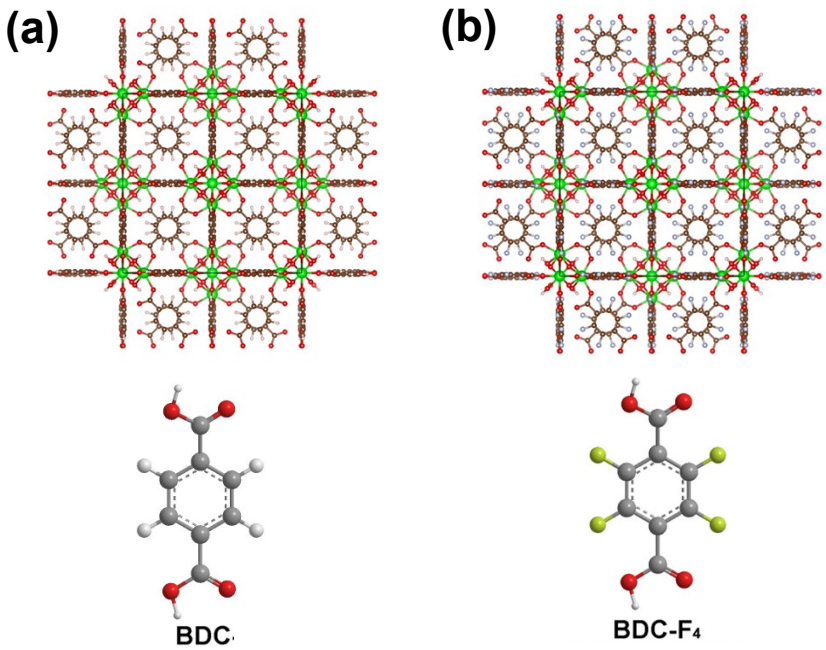

Figure S3. The crystal structure and the benzene-1,4-dicarboxylate (BDC) linkers of (a) UiO-66 and (b) UiO-66-F_4.

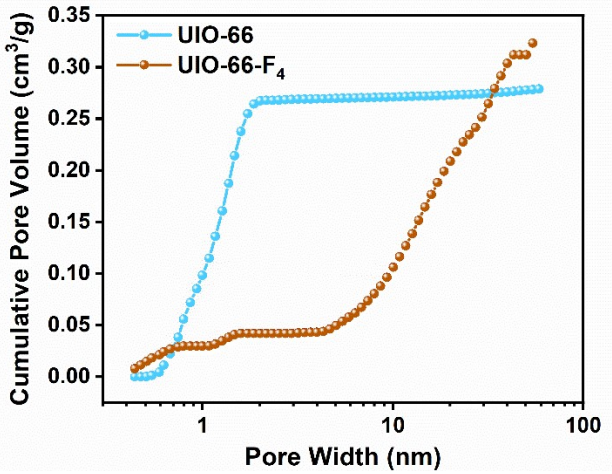

Figure S4. Cumulative volume of pores of UiO-66 and UiO-66-F_4.

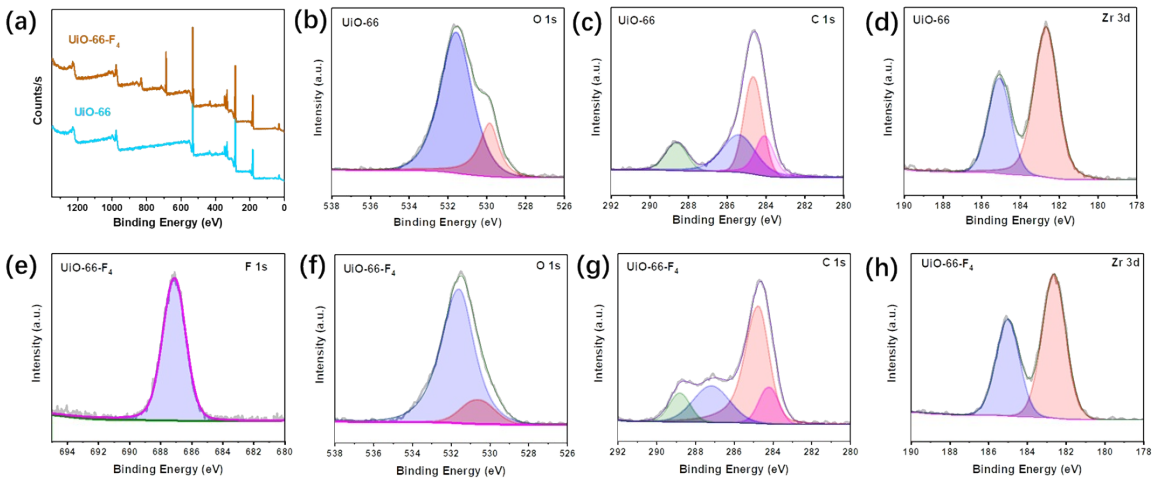

Figure S5. (a) XPS survey scan spectra of the UiO-66 and UiO-66-F_4. High resolution XPS spectra of the UiO-66: (b) O 1s, (c) C 1s, and (d) Zr 3d orbital. High resolution XPS spectra of the UiO-66-F_4: (e) F 1s, (f) O 1s, (g) C 1s, and (h) Zr 3d orbital.

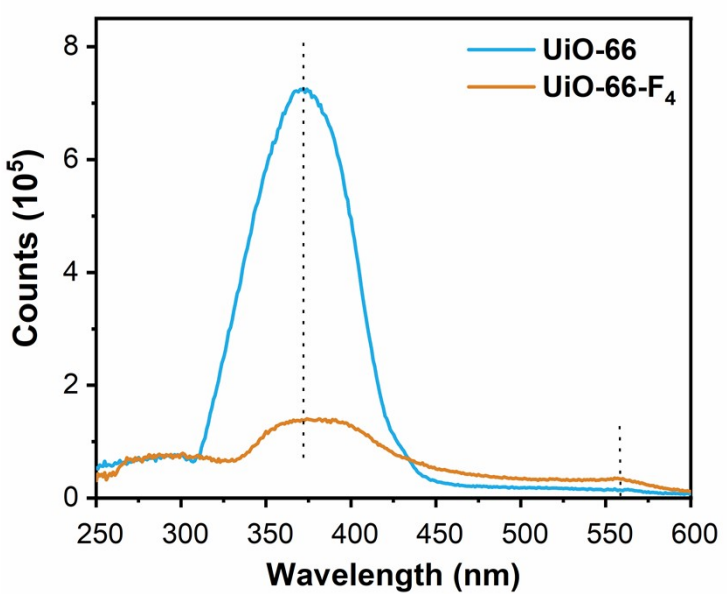

Figure S6. PL spetra of (a) UiO-66 and (b) UiO-66-F_4.

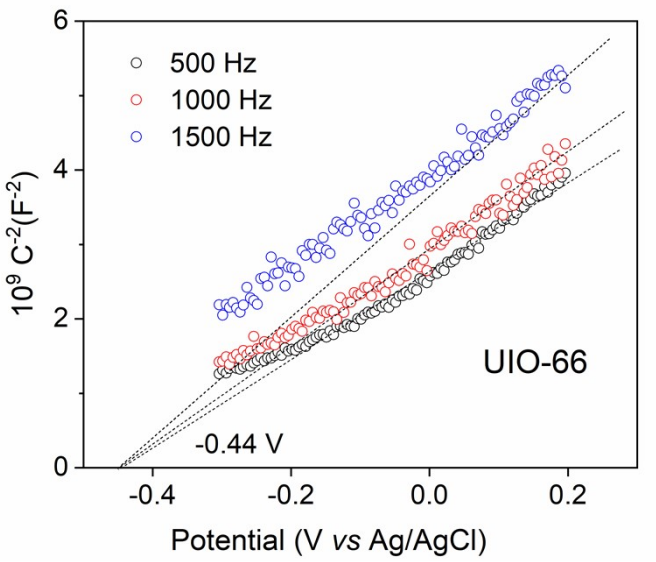

Figure S7. Mott-Schottky plots of the UiO-66 at different frequencies.

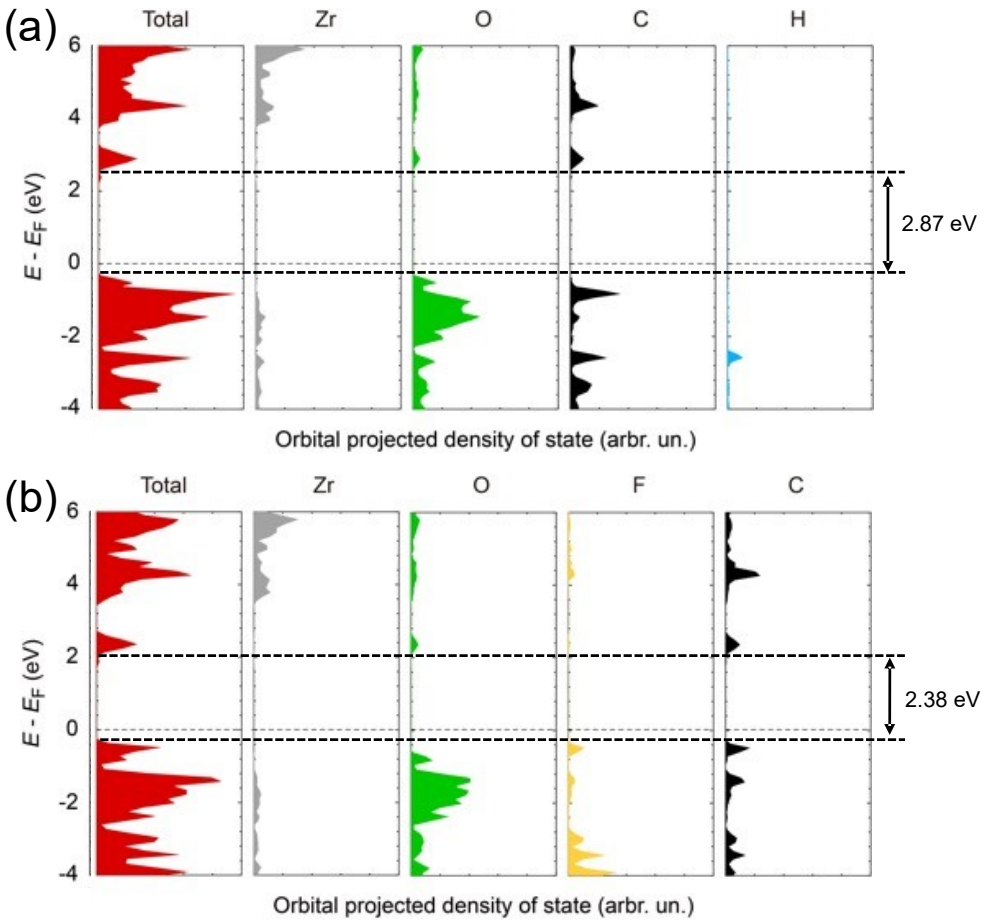

Figure S8. The calculated DOS results of (a) UiO-66 and (b) UiO-66-F_4.

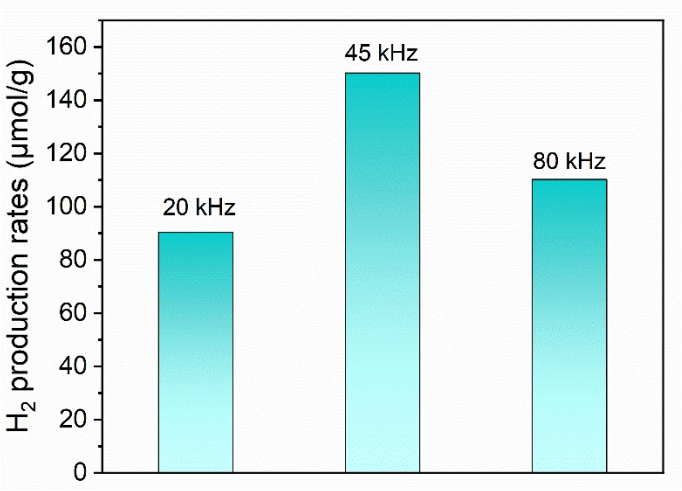

Figure S9. Comparison of H_2 production rates over UiO-66-F_4 nanosheets under different ultrasonic frequencies with an ultrasonic cleaner of KQ-100VDV (Kunshan Ultrasonic Instrument Co. Ltd.).

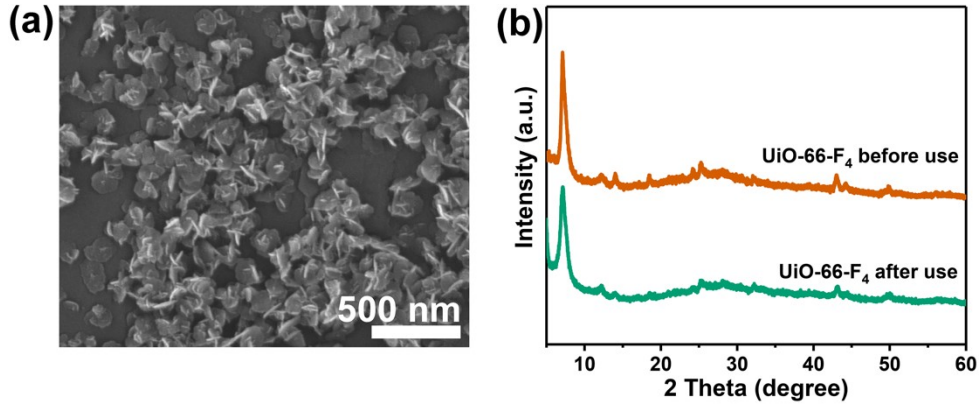

Figure S10. (a) The SEM image and (b) XRD patterns of the UiO-66-F_4 MOF after piezocatalytic H_2 production reactions for three cycles.

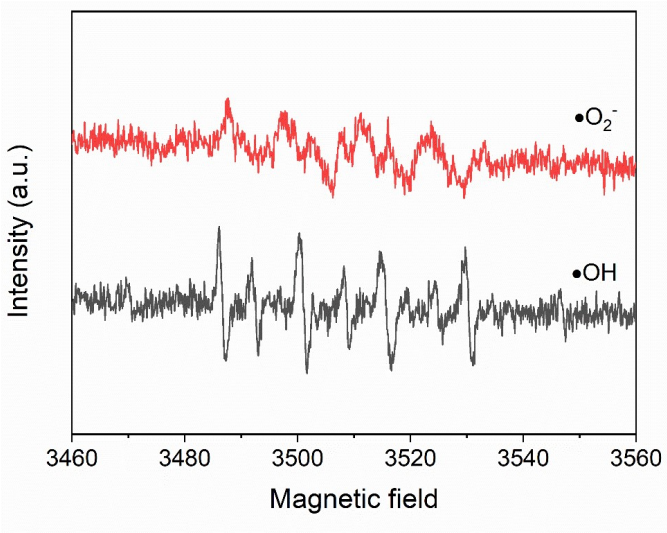

Figure S11. DMPO spin-trapping ESR spectra of the UiO-66-F_4 nanosheets in water (for DMPO-•OH) and in methanol (for DMPO-•O_2^-).